Accepted Manuscript

Construction of finite-dimensional multiresolutions based on linear subdivision schemes: Application to the 4-point shifted Lagrange scheme

Zhiqing Kui, Jean Baccou, Jacques Liandrat

PII: S0377-0427(18)30538-7
DOI: https://doi.org/10.1016/j.cam.2018.08.051
Reference: CAM 11888

To appear in: *Journal of Computational and Applied Mathematics*

Received date : 16 March 2018
Revised date : 23 August 2018

Please cite this article as: Z. Kui, J. Baccou, J. Liandrat, Construction of finite-dimensional multiresolutions based on linear subdivision schemes: Application to the 4-point shifted Lagrange scheme, *Journal of Computational and Applied Mathematics* (2018), https://doi.org/10.1016/j.cam.2018.08.051

Construction of Finite-dimensional Multiresolutions based on Linear Subdivision Schemes: Application to the 4-point Shifted Lagrange Scheme

Zhiqing KUI[a], Jean BACCOU[b], Jacques LIANDRAT[a]

[a] *Aix Marseille univ., CNRS, Centrale Marseille, I2M, UMR 7353, 13451 Marseille, France*
[b] *Institut de Radioprotection et de Sûreté Nucléaire(IRSN), PSN-RES/SEMIA/LIMAR, CE Cadarache, 13115 Saint Paul Les Durance, France*

Abstract

This paper is devoted to the construction of multiresolution frameworks related to general but linear subdivision schemes applied on sequences of finite length. Thanks to the flexible properties of subdivision schemes, a subdivision-based multiresolution is a promising powerful tool for compression, control and analysis of data. However, its construction is not straightforward neither for non-interpolatory subdivisions, nor for sequences of finite length. In this paper, given a subdivision for finite length sequences, we provide a first approach to construct compatible multiresolutions thanks to an extension of some classical wavelet results. As it will become clear that this type of approach can become computationally costly in practice, a new edge-adapted method that combines local consistent decimation is then developed to circumvent this limitation. An illustration in the case of the 4-point Shifted Lagrange subdivision scheme, for which there is no available multiresolution up to now, is then provided. Finally, some properties of the new multiresolutions are analysed and their performances are evaluated in the framework of image approximation.

Keywords: Multiresolution Analysis, Subdivision Scheme, Compatibility

1. Introduction

Multiresolution analyses are powerful tools in data approximation and analysis. Mimicking the framework of wavelets theory [1], multiresolution analyses have been recently constructed around uniform subdivision schemes in the linear and non-linear cases [2, 3]. For practical implementations, it is necessary to adapt to the interval the constructions on the infinite line. Considering the functional point of view, this led to wavelets theory on the interval [4] and many constructions [5]. Similarly, but taking the discrete point of view, this paper is devoted to the construction of multiresolution analyses for finite length sequences, starting, as in [3] from a given subdivision scheme. In this paper, we restrain our study to linear schemes.

A complete multiresolution analysis includes four schemes : the subdivision scheme, the decimation scheme and the detail subdivision and decimation schemes. These schemes must satisfy compatibility conditions in order to guaranty that the multiresolution decomposition of data is useful.

We first provide an extension of classical results coming from the wavelet framework to construct these four schemes without assuming the existence of any a priori known initial multi-scale basis. Then, since generally, subdivision schemes for finite length sequences are constructed from uniform schemes coupled with adaption at the beginning and the end of the sequences [6], we develop a new local multi-scale method that strongly reduces the computational cost of the first approach.

The paper is organized as follows. After an overview of discrete multiresolution analyses for finite length sequences (Section 2), the first construction of compatible multiresolutions (called global approach) is presented in Section 3. Section 4 is then devoted to the new local method to circumvent the limitation of

Email addresses: zhiqing.kui@centrale-marseille.fr (Zhiqing KUI), jean.baccou@irsn.fr (Jean BACCOU), jacques.liandrat@centrale-marseille.fr (Jacques LIANDRAT)

the first one. An illustration of these constructions is provided in Section 5 for the 4-point Shifted Lagrange scheme [7]. Section 6 is finally devoted to the application of the resulting multiresolutions in the framework of image non-linear approximation.

2. Multi-scale transforms of finite-dimensional data

We recall in this paper the construction of multi-scale transforms in the discrete framework also called Harten multiresolution [8]. In the context of finite-dimensional data, we use the formalism introduced in [9] even if the framework is completely different since NO initial multi-scale basis is a priori known or available. The general setting is defined by a family of triplets $(V^j, \tilde{H}^j, H^j)$ where $j \in \mathbb{Z}$ is a scale parameter, V^j denotes a separable space (finite-dimensional with $dim(V^j) = 2^j$ in our specific situation) associated to a resolution level 2^{-j}, $\tilde{H}^j$ (resp. H^j) is a decimation (resp. prediction) matrix connecting V^{j+1} to V^j (resp. V^j to V^{j+1}). The multiresolution is then fully specified by the introduction of a detail space W^j with $dim(W^j) = 2^j$ and two matrices $(\tilde{G}^j, G^j)$ connecting W^j and V^{j+1} such that $G^j : W^j \to V^{j+1}$, and $\tilde{G}^j : V^{j+1} \to W^j$.

For any integer j, a single scale decomposition can then be sketched as follows:

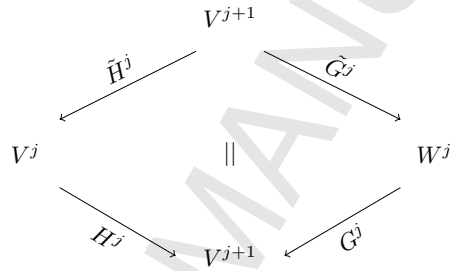

The quadruplet $(H^j, \tilde{H}^j, G^j, \tilde{G}^j)$ satisfies the reconstruction condition $H^j\tilde{H}^j + G^j\tilde{G}^j = I$ where I is the $2^{j+1} \times 2^{j+1}$ identity matrix. In this paper, we focus on **compatible** multiresolution which means that the quadruplet also verifies the following conditions:

$$\tilde{H}^j H^j = I,\ \tilde{G}^j G^j = I,\ \tilde{H}^j G^j = 0,\ \tilde{G}^j H^j = 0. \tag{1}$$

The first condition is the so-called **consistency** between prediction and decimation that will play a key role in the construction of decimation associated to a given subdivision.

Iterating the previous decomposition leads to the multi-scale decomposition of a sequence $f^j \in V^j$ denoted $\{f^{j_0}, d^{j_0}, d^{j_0+1}, ..., d^{j-1}\}$ with $j_0 < j$ and $d^i \in W^i, j_0 \le i \le j-1$:

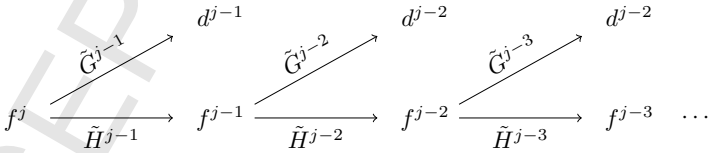

Similarly, a multi-scale reconstruction consists in recovering f^j from $\{f^{j_0}, d^{j_0}, d^{j_0+1}, ..., d^{j-1}\}$ thanks to H^j and G^j:

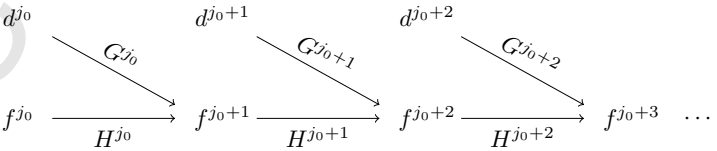

The next two sections are devoted to the construction of the quadruplets $(H^j, \tilde{H}^j, G^j, \tilde{G}^j)$. For wavelet multiresolution analysis of $L^2(\mathbb{R})$ [1], these matrices are completely specified by the choice of scaling functions and wavelets. However, in a more general framework, such a construction is not always straightforward. A formal approach has been developed in [5] for bounded domains when the prediction is obtained from a refinement relation between functions. It exploits the notion of stable completion (involving compactly supported functions) that allows to derive a decimation matrix. In the next section, we revisit this approach from a discrete point of view i.e. without assuming the existence of a priori known functions. In this case, the key ingredient is a consistency relation between prediction and decimation.

3. Construction of compatible multiresolutions: an extension of the wavelet approach

We first propose in the sequel a generic approach based on matrix manipulations to exhibit, given a matrix H^j, a consistent matrix $\tilde{H}^j$ (i.e satisfying the first equality of (1)). Then, given a couple of consistent matrices $(H^j, \tilde{H}^j)$, we focus on the construction of compatible G^j and $\tilde{G}^j$.

3.1. Notations

Before providing the main results, we first define some notations. For sake of clarity, we remove the scale label. The matrix O (resp. E) corresponds to the odd (resp. even) subsampling, i.e: $\forall f, \forall k, (Of)_k = f_{2k+1}$ (resp. $(Ef)_k = f_{2k}$). Moreover, C stands for the square interlacing defined by $\forall f, f = C \begin{bmatrix} Of \\ Ef \end{bmatrix}$.

3.2. Decimation matrix

The following proposition holds:

Proposition 1 (Construction of $\tilde{H}^j$)**.** *Given a prediction matrix H^j such that OH^j and EH^j are invertible. Denoting Λ a square matrix, then*

$$\tilde{H}^j = \Lambda(OH^j)^{-1}O + (I - \Lambda)(EH^j)^{-1}E \tag{2}$$

defines a decimation matrix consistent with H^j.

Proof. The proof is straightforward since

$$H^j = C \begin{bmatrix} OH^j \\ EH^j \end{bmatrix},$$

then $\tilde{H}^j H^j = \Lambda + (I - \Lambda) = I$.

□

The construction (2) is based on a combination of matrices that operate on odd and even terms of the sequence to be decimated. Thanks to Λ (resp. $I - \Lambda$) that controls the contribution of odd (resp. even) part, it leads to a large choice of decimation matrices. Without any assumption on H^j, one might consider that the odd part and even parts should have the same influence and take $\Lambda = \frac{1}{2}I$, this will be true in the example of this paper.

3.3. Compatible detail matrices

Starting from $(H^j, \tilde{H}^j)$, compatible G^j and $\tilde{G}^j$ can be constructed according to the following proposition derived in [3].

Proposition 2 (Construction of G^j and $\tilde{G}^j$)**.** *If $\tilde{H}^j E'$ is invertible, then*

$$\begin{cases} \tilde{G}^j = O(I - H^j\tilde{H}^j) \\ G^j = C \begin{bmatrix} I \\ -(\tilde{H}^j E')^{-1}\tilde{H}^j O' \end{bmatrix}, \end{cases} \tag{3}$$

are compatible with $(H^j, \tilde{H}^j)$.

The approach described in this section is global in the sense that it leads, in one step, to the matrix that specifies the decimation rule for every element of any finite sequence $f^{j+1} \in V^{j+1}$. It is important to mention that there is no underlying functions in this construction. Therefore, the results stated by Propositions 1 and 2 encompass the construction performed in the wavelet framework.

However, for each j, the inversion of two matrices of size $2^j \times 2^j$ is required. This can be computationally costly for large j and reduce the efficiency of the global approach for large datasets. In the next section, we focus on the specific situation where H^j is constructed using a subdivision with adaption at the edges. We develop a new method that exploits the local property of the subdivision-based prediction and allows to reduce the complexity.

4. Construction of compatible multiresolutions: a new local approach

The starting point of the method is the local adaption of the subdivision scheme. This is recalled in the next section. It is then exploited to derive an original construction of a decimation matrix without inverting large size matrices as in Proposition 1.

4.1. Construction of the prediction matrix

A uniform subdivision operator h [10] is defined through a real-valued sequence $(h_k)_{k\in\mathbb{Z}}$ having a finite number of non-zero values such that $(f_k)_{k\in\mathbb{Z}} \in l^\infty(\mathbb{Z}) \mapsto ((hf)_k)_{k\in\mathbb{Z}} \in l^\infty(\mathbb{Z})$ with

$$(hf)_k = \sum_{l\in\mathbb{Z}} h_{k-2l} f_l \ . \tag{4}$$

A set $\{h_k : k_0 \leq k \leq k_1, k \in \mathbb{Z}\}$ containing all the non-zero values of $(h_k)_{k\in\mathbb{Z}}$ is called a mask of the subdivision. In the sequel, we restrict our study to symmetric schemes with a mask of length $2n$ ($n \geq 2$) that is written

$$\{h_{-n}, h_{-n+1}, \ldots, h_{n-2}, h_{n-1}\}. \tag{5}$$

Moreover, we define the prediction stencil associated to the index k. It is computed from (4) as the set of index $\mathcal{I}_k = \{l \in \mathbb{Z} : h_{k-2l} \neq 0\}$. This set contains at most n elements and depends on the parity of k.

In the subdivision framework, the coefficients of the mask are used to construct the prediction matrix. On the line, the prediction matrix is infinite. In the case of finite-dimensional data, the subdivision rule has to be adapted for the treatment of the first and last elements of the finite length sequence. This type of adaption has been already addressed in [6] in the case of the development of a position-dependent approach in the interpolatory (Lagrange, [7]) framework. It led to modified subdivisions schemes that take into account the presence of segmentation points in the data. The key idea of this modification relied on a modification of the prediction stencil and the related coefficients. More precisely, the prediction of $f^{j+1} = \{f_1^{j+1}, f_2^{j+1}, \ldots, f_{2^{j+1}}^{j+1}\} \in V^{j+1}$ from $f^j = \{f_1^j, f_2^j, \ldots, f_{2^j}^j\} \in V^j$ was based on the following position-dependent stencil selection[1].

Definition 1 (Position-dependent stencil selection)**.** *For any $k \in \{1, \ldots, 2^{j+1}\}$, the position-dependent prediction stencil I_k^{j+1} is defined by:*

$$I_k^{j+1} = \begin{cases} \{1, \ldots, n\} \text{ if } \mathcal{I}_k \cap \{l \in \mathbb{Z} : l < 1\} \neq \emptyset, \\ \{2^j - n + 1, \ldots, 2^j\} \text{ if } \mathcal{I}_k \cap \{l \in \mathbb{Z} : l > 2^j\} \neq \emptyset, \\ \mathcal{I}_k \text{ otherwise.} \end{cases} \tag{6}$$

[1] In this construction, it is always assumed that j is sufficiently large to allow both uniform prediction (in the inner part of the interval) and adaption (at the edges).

This type of approach (which is not reduced to the interpolatory framework) is also followed in the sequel.

Besides the classical refinement matrices [7] associated to uniform subdivision scheme, this adaption leads to the introduction of two edge matrices [6] M_0 and M_1 to describe the prediction of the edge elements. Indeed, there exist two matrices of dimension $n \times n$ such that

$$\begin{bmatrix} f_1^{j+1} \\ f_2^{j+1} \\ \vdots \\ f_n^{j+1} \end{bmatrix} = M_0 \begin{bmatrix} f_1^{j} \\ f_2^{j} \\ \vdots \\ f_n^{j} \end{bmatrix}, \quad \begin{bmatrix} f_{2^{j+1}-n+1}^{j+1} \\ f_{2^{j+1}-n+2}^{j+1} \\ \vdots \\ f_{2^{j+1}}^{j+1} \end{bmatrix} = M_1 \begin{bmatrix} f_{2^j-n+1}^{j} \\ f_{2^j-n+2}^{j} \\ \vdots \\ f_{2^j}^{j} \end{bmatrix} . \tag{7}$$

According to the stencil, the last row of M_0 and the first row of M_1 are given by the uniform subdivision (5). The prediction matrix H^j is finally constructed by combining the previous edge matrices with the matrix associated to the uniform prediction. Its structure (only the non-zero coefficients are provided) is illustrated below when $n = 4$:

$$\begin{bmatrix}
\circ & \circ & \circ & \circ & & & & \\
\circ & \circ & \circ & \circ & & & & \\
\circ & \circ & \circ & \circ & & & & \\
\odot & \odot & \odot & \odot & & & & \\
\cdot & \cdot & \cdot & \cdot & & & & \\
 & \cdot & \cdot & \cdot & \cdot & & & \\
 & \cdot & \cdot & \cdot & \cdot & & & \\
 & & \cdot & \cdot & \cdot & \cdot & & \\
 & & \cdot & \cdot & \cdot & \cdot & & \\
 & & \ddots & \ddots & \ddots & \ddots & & \\
 & & & \cdot & \cdot & \cdot & \cdot & \\
 & & & \cdot & \cdot & \cdot & \cdot & \\
 & & & & \cdot & \cdot & \cdot & \cdot \\
 & & & & \odot & \odot & \odot & \odot \\
 & & & & \circ & \circ & \circ & \circ \\
 & & & & \circ & \circ & \circ & \circ \\
 & & & & \circ & \circ & \circ & \circ
\end{bmatrix},$$

where the symbol $\circ$ stands for the coefficients of M_0 and M_1 and the symbol $\cdot$ stands for the non-zero coefficients of the matrix associated to the uniform subdivision. The first and last row of M_0 and M_1 are also constructed by uniform subdivision, that is why their coefficients are represented by the symbol $\odot$.

4.2. Construction of the decimation matrix and of the full compatible multiresolution

A decimation matrix can also be derived from a uniform decimation operator adapting it at the edges.

A uniform decimation operator $\tilde{h}$ is defined through a real-valued sequence $(\tilde{h}_k)_{k\in\mathbb{Z}}$ having a finite number of non-zero values such that $(f_k)_{k\in\mathbb{Z}} \in l^\infty(\mathbb{Z}) \mapsto ((\tilde{h}f)_k)_{k\in\mathbb{Z}} \in l^\infty(\mathbb{Z})$ with

$$(\tilde{h}f)_k = \sum_{l\in\mathbb{Z}} \tilde{h}_{l-2k} f_l \ . \tag{8}$$

When the subdivision operator is given, the construction of consistent uniform decimation operators (on the line) has been tackled in [2] by introducing a generic method. It is recalled in the following :

Lemma 1. *Let h be a uniform subdivision operator given by (5). Introducing the square matrix of dimension $2(n-1)\times 2(n-1)$*

$$M=\begin{bmatrix} h_{n-2} & h_{n-4} & \cdots & h_{-n} & 0 & \cdots & 0\\ h_{n-1} & h_{n-3} & \cdots & h_{-n+1} & 0 & \cdots & 0\\ 0 & h_{n-2} & h_{n-4} & \cdots & h_{-n} & \cdots & 0\\ 0 & h_{n-1} & h_{n-3} & \cdots & h_{-n+1} & \cdots & 0\\ \vdots & & & \vdots & & & \\ 0 & 0 & \cdots & h_{n-2} & h_{n-4} & \cdots & h_{-n}\\ 0 & 0 & \cdots & h_{n-1} & h_{n-3} & \cdots & h_{-n+1} \end{bmatrix}.$$

If $det(M)\neq 0$, there exists $2(n-1)$ **elementary** *consistent decimation operators the mask of which are of length $2(n-1)$. They are given by each row of M^{-1}:*

$$M^{-1}=\begin{bmatrix} \tilde{h}^{(1)}_{n-2} & \tilde{h}^{(1)}_{n-1} & \cdots & \tilde{h}^{(1)}_{3n-5}\\ \tilde{h}^{(2)}_{n-4} & \tilde{h}^{(2)}_{n-3} & \cdots & \tilde{h}^{(2)}_{3n-7}\\ \vdots & & \vdots & \\ \tilde{h}^{(2n-2)}_{-3n+4} & \tilde{h}^{(2n-2)}_{-3n+5} & \cdots & \tilde{h}^{(2n-2)}_{-n+1} \end{bmatrix}.$$

Moreover, all the consistent uniform decimation operators can be constructed as

$$\sum_{t\in\mathcal{T}}\sum_{i\in\mathcal{I}} c_{i,t}T_{2t}(\tilde{h}^{(i)}) \tag{9}$$

with

$$\forall t\in\mathcal{T}\subset\mathbb{Z},\ \sum_{i\in\mathcal{I}} c_{i,t}=\delta_{t,0},\ \ and\ \ \ 0\in\mathcal{T}\ ,$$

where, for any decimation operator $\tilde{h}$ and any integer t, $T_t(\tilde{h})$ is the decimation operator related to the sequence $(\tilde{h}_{k-t})_{k\in\mathbb{Z}}$.

The large choice of decimation operators offered by this approach is of prime importance in practice since it allows to reach specific characteristics of the scheme according to given objectives. Finite length management, addressed in this paper, is an example: in this case, the construction of consistent decimation can be performed following the next proposition.

Proposition 3. *Let H^j be a prediction matrix constructed following Section 4.1. If $det(M_0)\cdot det(M_1)\neq 0$, a consistent decimation matrix $\tilde{H}^j$ can be obtained by combining M^{-1}, M_0^{-1} and M_1^{-1}.*

Proof. Exploiting Lemma 1, elementary decimations can be used to map $\{f_n^{j+1},\dots,f_{2^{j+1}-n+1}^{j+1}\}$ to $\{f_n^j,\dots,f_{2^j-n+1}^j\}$. Indeed, choosing correctly the elementary decimations among the lines of M^{-1}, when $n\geq 2$, the first (resp. last) element f_n^j (resp. $f_{2^j-n+1}^j$) can be computed using an elementary decimation scheme (8) involving $\{f_l^{j+1}\}_{l=n,\dots,3n-3}$ (resp. $\{f_l^{j+1}\}_{l=2^{j+1}-3n+4,\dots,2^{j+1}-n+1}$).

Moreover, according to (7), M_0^{-1} and M_1^{-1} lead to consistent decimations for the n first and n last elements of f^{j+1}. Since the position-dependent stencil selection (Definition 1) ensures that the last and first rows of M_0 and M_1 correspond to a uniform subdivision, one can construct a consistent $\tilde{H}^j$ according to the following decimation process described for simplicity for the left hand side of the data,

□

If one wants to use a non elementary decimation (Expression (9) of Lemma 1) for the inner part of the interval, the previous construction can be adapted by specifying the decimation process as follows (only the treatment of the left hand side data is described):

- Decimation of $\{f_1^{j+1},\dots,f_{n-1}^{j+1}\}$ involving rows of M_0^{-1},

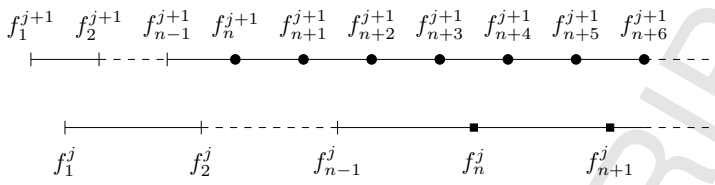

Figure 1: Consistent decimation process of a finite length sequence. The black disks stand for the elements subdivided using a uniform subdivision and the black squares are associated to a uniform decimation. The remaining elements are obtained using a position-dependent strategy involving rows of M_0^{-1}.

- Decimation of $\{f_n^{j+1}, \ldots, f_{2^{j+1}-n+1}^{j+1}\}$ involving
  - an elementary decimation from M^{-1} if $\{f_n^{j+1}, \ldots, f_{2^{j+1}-n+1}^{j+1}\}$ is not mapped to $\{f_n^j, \ldots, f_{2^j-n+1}^j\}$ when using the decimation constructed from (9),
  - the decimation constructed from (9) otherwise.

This approach leads to a sparse $\tilde{H}^j$ which is composed of different blocks associated to position-dependent or uniform consistent decimations. Its structure is illustrated below by the sketch of the matrix that corresponds to $n = 4$ and therefore to elementary decimation operators of length 6 according to Lemma 1. In this sketch, we assume that a uniform decimation of length 8 is used in the inner part of the interval. This is the situation that will be considered in the numerical tests.

Similarly to the previous section, we only provide the non-zero coefficients with the following conventions: the symbol $\circ$ represents the coefficients of M_0^{-1} and M_1^{-1}, the symbol $\odot$ denotes the coefficients of the elementary decimation and the symbol $\cdot$ is associated to the uniform decimation of length 8.

From this band matrix $\tilde{H}^j$, the complete multiresolution can be derived following Proposition 2. Here, $\tilde{G}^j$ is a band matrix as well as $(\tilde{H}^j E')$. Therefore, application of G^j requires $O(2^j)$ operations.

5. Application to the 4-point Shifted Lagrange scheme

An example of construction of a compatible multiresolution following the edge-adapted approach (referred as *the local approach*) is given in the sequel. It involves the 4-point Shifted Lagrange Scheme [7] for which there is up to now no available consistent decimation in the case of finite-dimensional data. A comparison with the global approach of Section 3 is also provided. A special attention is devoted to the construction of the matrices $\tilde{H}^j$, $\tilde{G}^j$ and G^j that controls the efficiency of the implementation of the methods in practice.

5.1. Prediction matrix

The 4-point Shifted Lagrange Scheme is defined by sampling the interpolating Lagrange polynomial of degree 3 associated to the stencil $\{-1, 0, 1, 2\}$ at positions $\{1/4, 3/4\}$. Its mask is given by

$$\{h_{-4}, h_{-3}, h_{-2}, h_{-1}, h_0, h_1, h_2, h_3\} = \{-\frac{5}{128}, -\frac{7}{128}, \frac{35}{128}, \frac{105}{128}, \frac{105}{128}, \frac{35}{128}, -\frac{7}{128}, -\frac{5}{128}\}. \tag{10}$$

Up to now, the construction of the scheme has been performed on the real line. We propose in the sequel an adaption of the prediction rule to take into account finite length sequences.

Following Section 4.1, one can define edge matrices by shifting the stencil for the prediction of the first and last elements of the finite length sequence. In this example, it is equivalent to consider the same stencil as before and to change the sampling points that are now $(-5/4, -3/4, -1/4)$ and $(5/4, 7/4, 9/4)$. The resulting matrices M_0 and M_1 are:

$$M_0 = \begin{bmatrix} 195/128 & -117/128 & 65/128 & -15/128 \\ 77/128 & 77/128 & -33/128 & 7/128 \\ 15/128 & 135/128 & -27/128 & 5/128 \\ -7/128 & 105/128 & 35/128 & -5/128 \end{bmatrix}, \quad M_1 = \begin{bmatrix} -5/128 & 35/128 & 105/128 & -7/128 \\ 5/128 & -27/128 & 135/128 & 15/128 \\ 7/128 & -33/128 & 77/128 & 77/128 \\ -15/128 & 65/128 & -117/128 & 195/128 \end{bmatrix}.$$

The prediction matrix H^j is finally written as

$$H^j = \begin{bmatrix} 195/128 & -117/128 & 65/128 & -15/128 & 0 & 0 & \cdots \\ 77/128 & 77/128 & -33/128 & 7/128 & 0 & 0 & \cdots \\ 15/128 & 135/128 & -27/128 & 5/128 & 0 & 0 & \cdots \\ -7/128 & 105/128 & 35/128 & -5/128 & 0 & 0 & \cdots \\ -5/128 & 35/128 & 105/128 & -7/128 & 0 & 0 & \cdots \\ 0 & -7/128 & 105/128 & 35/128 & -5/128 & 0 & \cdots \\ 0 & -5/128 & 35/128 & 105/128 & -7/128 & 0 & \cdots \\ & \ddots & & \ddots & & \ddots & \end{bmatrix}. \tag{11}$$

The complete matrix H^j is shown in the appendix for $j = 3$.

5.2. Consistent Decimation Matrices

If the local approach of Section 4 is applied, it is not required to invert H^j. Moreover, $\tilde{H}^j$ can be obtained by combining position-dependent and uniform decimations: position-dependent decimation is defined from the rows of M_0^{-1} and M_1^{-1} :

$$M_0^{-1} = \begin{bmatrix} 5/16 & 15/16 & -5/16 & 1/16 \\ 1/16 & -5/16 & 15/16 & 5/16 \\ -35/16 & 135/16 & -189/16 & 105/16 \\ -231/16 & 819/16 & -1001/16 & 429/16 \end{bmatrix}, \quad M_1^{-1} = \begin{bmatrix} 429/16 & -1001/16 & 819/16 & -231/16 \\ 104/16 & -189/16 & 135/16 & -35/16 \\ 5/16 & 15/16 & -5/16 & 1/16 \\ 1/16 & -5/16 & 15/16 & 5/16 \end{bmatrix}.$$

Concerning the uniform decimation, we exploit the generic method recalled in Lemma 1 and focus on a decimation operator consistent with (10) of mask of length 8 that led to promising results in [3] for image approximation. Its mask is given by:

$$\{\tilde{h}_{-4}, \tilde{h}_{-3}, \tilde{h}_{-2}, \tilde{h}_{-1}, \tilde{h}_0, \tilde{h}_1, \tilde{h}_2, \tilde{h}_3\} = \{\frac{95}{2304}, -\frac{133}{2304}, -\frac{35}{256}, \frac{1505}{2304}, \frac{1505}{2304}, -\frac{35}{256}, -\frac{133}{2304}, \frac{95}{2304}\}. \tag{12}$$

According to the local method of Section 4.2, we obtain the following consistent decimation matrix, combining M_0^{-1}, M_1^{-1} and (12):

$$\begin{bmatrix} 5/16 & 15/16 & -5/16 & 1/16 & 0 & 0 & \cdots \\ 1/16 & -5/16 & 15/16 & 5/16 & 0 & 0 & \cdots \\ -35/16 & 135/16 & -189/16 & 105/16 & 0 & 0 & \cdots \\ 0 & 0 & 0 & 95/2304 & -133/2304 & -35/256 & \cdots \\ & \ddots & & \ddots & & \ddots & \end{bmatrix}.$$

In this example, we can also substitute the third (and similarly the $2^j - 2$) row of $\tilde{H}^j$ with a uniform decimation since the consistency still holds. Then we get:

$$\tilde{H}^j = \begin{bmatrix} 5/16 & 15/16 & -5/16 & 1/16 & 0 & 0 & \cdots \\ 1/16 & -5/16 & 15/16 & 5/16 & 0 & 0 & \cdots \\ 0 & 95/2304 & -133/2304 & -35/256 & 1505/2304 & 1505/2304 & \cdots \\ 0 & 0 & 0 & 95/2304 & -133/2304 & -35/256 & \cdots \\ & \ddots & & \ddots & & \ddots & \end{bmatrix}. \tag{13}$$

The complete decimation matrix (13) is given in the appendix when $j = 3$.

Remark 1. *The previous substitution is possible since, by construction, the prediction associated to M_0 corresponds to the same Lagrange polynomial of degree 3 evaluated at different positions. It is therefore possible to predict f_2^{j+1} and f_3^{j+1} with a uniform (centered) stencil from the sampling of the same polynomial. This can be achieved by artificially introducing one extra element resulting from the extrapolation of the polynomial constructed from $\{f_1^j, f_2^j, f_3^j, f_4^j\}$. More generally, it points out that, similarly to the uniform construction, there exists different choices to define the adaption of the decimation. The question of an optimal construction is out of the scope of this paper.*

For sake of comparison, we also provide in the appendix the decimation matrix derived from the global method following Proposition 1 for $\Lambda = \frac{1}{2}I$.

Following Proposition 2, the detail matrices are finally constructed and are given in the appendix. As expected, $\tilde{G}^j$ exhibits a band structure.

6. Numerical results

We numerically study the performance of the previous multi-scale transforms in terms of stability, computational time to construct them and image approximation capability.

6.1. Stability

For practical issues, a key property of multi-scale transforms is their stability. We refer to [8] for a precise definition. It is directly connected to the stability of the prediction and decimation transforms that reads:

Definition 2. *The prediction transform associated to the family of matrices $\{H^j\}_{j\geq j_0}$ is stable with regards to the norm $||\ .\ ||$ if there exists a constant C_0 such that*

$$\forall j > j_0, \quad ||H^j H^{j-1} \cdots H^{j_0}|| \leq C_0.$$

The decimation transform associated to the family of matrices $\{\tilde{H}^j\}_{j\geq j_0}$ is stable with regards to the norm $||\ .\ ||$ if there exists C_0 such that

$$\forall j_0 < j, \quad ||\tilde{H}^{j_0} \tilde{H}^{j_0+1} \cdots \tilde{H}^j|| \leq C_0.$$

There exist several results related to the stability of linear multiresolutions on the real line [8]. They are connected to the convergence of the subdivision scheme when focussing on the reconstruction transform. Concerning the decomposition one, the stability issue is more involved but a theoretical result has been proposed in [3] for any consistent decimations. However, the question still remains open in the case of finite length sequences. Therefore, the numerical tests are restricted in the sequel to the study of the behavior of the two following quantities according to Definition 2:

$$\forall i \in \mathbb{N}, \quad S_i^{j_0} = H^{j_0+i} H^{j_0+i-1} \cdots H^{j_0},$$

and

$$\forall i \in \mathbb{N}, \quad \tilde{S}_i^{j_0} = \tilde{H}^{j_0-i} \tilde{H}^{j_0-i+1} \cdots \tilde{H}^{j_0},$$

where j_0 is the initial scale.

Using (11) we get the following evaluation of $||S_i^2||_\infty$ (Figure 2), which indicates that the subdivision is numerically stable.

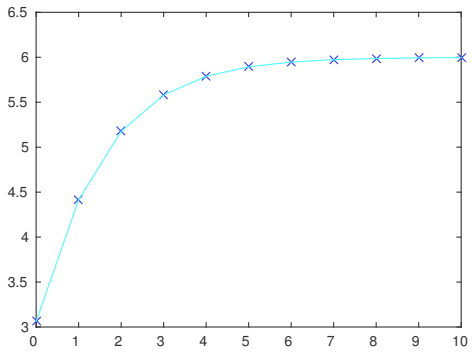

Figure 2: Stability of the subdivision transform, $||S_i^2||_\infty$ versus i

Concerning the stability of the decimation, Figure 3 displays the value of $||\tilde{S}_0^j||_\infty = ||\tilde{H}^j||_\infty$ for $4 \leq j \leq 13$ and $||\tilde{S}_i^{13}||_\infty$ for $0 \leq i \leq 8$ where the decimation matrix is given by (13) for the edge-adapted method and by (2) with $\Lambda = \frac{1}{2}I$ for the global one. The numerical stability of decimations is deduced by two observations: $||\tilde{S}_0^j||_\infty$ is numerically constant for large values of j (left), and $||\tilde{S}_i^j||_\infty$ tends to stabilize for large i (right) around numerically acceptable constants.

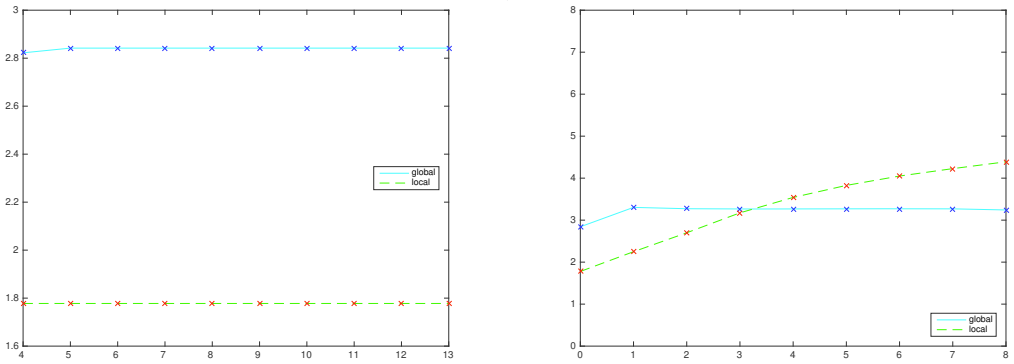

Figure 3: Stability of global/local decimation transforms, Left : $||\tilde{S}_0^j||_\infty$ versus j Right : $||\tilde{S}_i^{13}||_\infty$ versus i;

Both approaches therefore lead to numerically stable decimations.

6.2. Computational cost

For practical issues, it is also interesting to compare the two approaches in term of CPU time related to the implementation of the associated multi-scale transforms. Since the matrix G^j and $\tilde{G}^j$ are used in both methods according to Proposition 2, this numerical study is reduced to the evaluation of the CPU time associated to $\tilde{H}^j$.

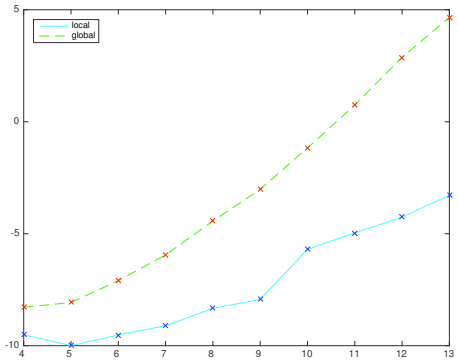

Figure 4: CPU time for the construction of a consistent decimation matrices $\tilde{H}^j$ versus scale j ($\log_2$-scale)

Figure 4 displays the evolution of the CPU time for each construction versus the scale. The edge-adapted approach leads to a significant reduction of the computational time with a factor varying from 2 (small values of j) to 200 (large values of j). For large values of j, the local approach should be preferred to the global one.

6.3. Image approximation

Finally, we evaluate the properties of both approaches in the framework of image processing. For sake of completeness in this study, we also consider the multiresolution associated to the classical 4-point interpolatory Lagrange scheme [11] (combined with the consistent subsampling decimation).

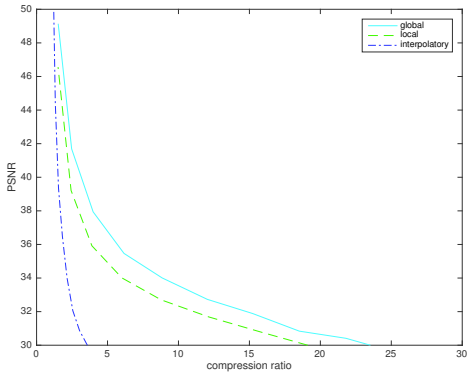

Figure 5: Left: test image *pepper*; Right: PSNR versus compression ratio for Shifted Lagrange (local and global method for the construction of the decimation matrix) and interpolatory multiresolutions (subsampling decimation).

Starting from an image of size 512×512 ($j = 9$), several decompositions are performed until $j_0 = 5$. Then after truncation of the detail coefficients according to a certain threshold, the reconstruction transform is applied and the resulting image is compared to the original one by computing the so-called PSNR (Peak Signal-to-Noise Ratio) which indicates the quality of the reconstructed image. Figure 5 displays the evolution of the PSNR with respect to the compression ratio (i.e. ratio between the size of the original image and the size of the compressed image).

As already noticed in [3], Figure 5 first exhibits that shifted multiresolutions (that are non-interpolatory) outperform the interpolatory one. Moreover, when comparing local and global approaches, it appears that the second one leads to a better result with an improvement of the compression ratio to reach a fixed PSNR.

This last result combined with the numerical study of Section 6.2 tends to indicate that a compromise has to be found in practice. By construction, the local method involves (sparse) matrix structures that are more convenient to handle and can be performed with an affordable computational cost for any scale. If the user accepts to increase the complexity of the multi-scale algorithms and focusses on sequences that are not too long, the previous results show that the global approach can improve the compression performance. An efficient strategy could be to design non-stationary schemes using global approach for small values of j and local approach otherwise.

7. Conclusion

We have presented constructions of consistent decimation operators associated to linear subdivision schemes for finite length sequences. Two approaches have been proposed : the first one, based on even/odd subsampling provides a global (full matrix) approach, while the second one exploits the adaption of the subdivision at the edges of sequences and provides a local (band matrix) decimation. From these operators, associated detail schemes, derived adapting the general approach on the line, have been constructed. Applications to the Shifted Lagrange subdivision scheme adapted to finite length sequences have been given as examples. Numerical tests in the framework of image non-linear approximation showed that the resulting new multiresolutions may compare favorably with already existing constructions.

Further works concern the theoretical analysis of the stability of the multiresolutions. The contributions provided in this paper in the linear case should also be extended to other situations. It includes, in particular, a full construction of multiresolutions in the non-linear framework. Such a construction has been already performed for subdivisions defined on the real line [3]. For finite length sequence, the two approaches introduced in this paper can be exploited. However, it first requires modifying the non-linear subdivision rule for the treatment of the first and last elements of the sequence. If the local approach is followed, the consistency of the decimation constructed by combining local decimations (inversion of edge matrices) and uniform ones (derived from the method proposed in [3]) should also be checked.

References

[1] I. Daubechies, Ten lectures on wavelets, SIAM, Philadelphia, 1992.

[2] Z. Kui, J. Baccou, J. Liandrat, On the coupling of decimation operator with subdivision schemes for multi-scale analysis, in: Lecture Notes in Comput. Sci., Vol. 10521, Springer, 2016, pp. 162–185.

[3] Z. Kui, On the construction of multiresolution analysis compatible with general subdivisions, Ph.D. thesis, Ecole Centrale de Marseille (2018).

[4] A. Cohen, I. Daubechies, P. Vial, Wavelet bases on the interval and fast algorithms, Appl. Comput. Harmon. Anal. 1 (1993) 54–81.

[5] W. Dahmen, A. Kunoth, K. Urban, Biorthogonal spline-wavelets on the interval - stability and moment conditions, Appl. Comp. Harm. Anal. 6 (1997) 132–196.

[6] J. Baccou, J. Liandrat, Position-dependent lagrange interpolating multiresolutions, International journal of wavelets, multiresolution and information processing 5 (04) (2007) 513–539.

[7] N. Dyn, M. S. Floater, K. Hormann, A C^2 four-point subdivision scheme with fourth order accuracy and its extensions, in: Mathematical Methods for Curves and Surfaces: Tromsø 2004, Modern Methods in Mathematics, Citeseer, Nashboro Press, 2005, pp. 145–156.

[8] A. Harten, Multiresolution representation of data: A general framework, SIAM J. Numer. Anal. 33 (3) (1996) 1205–1256.

[9] J. M. Carnicer, W. Dahmen, J. M. Peña, Local decomposition of refinable spaces and wavelets, Appl. Comput. Harmon. Anal. 3 (2) (1996) 127–153.

[10] N. Dyn, Subdivision schemes in computer aided geometric design, in: Light, W.(ed.) Advances in Numerical Analysis II, Wavelets, Subdivision Algorithms and Radial Functions, Clarendon Press, Oxford, 1992, pp. 36–104.

[11] N. Dyn, D. Levin, J. A. Gregory, A 4-point interpolatory subdivision scheme for curve design, Computer aided geometric design 4 (4) (1987) 257–268.

Appendix

Prediction matrix associated to the 4-point Shifted Lagrange subdivision scheme for $j = 3$,

$$H^3 = \begin{bmatrix} \frac{195}{128} & -\frac{117}{128} & \frac{65}{128} & -\frac{15}{128} & 0 & 0 & 0 & 0 \\ \frac{77}{128} & \frac{77}{128} & -\frac{33}{128} & \frac{7}{128} & 0 & 0 & 0 & 0 \\ \frac{15}{128} & \frac{135}{128} & -\frac{27}{128} & \frac{5}{128} & 0 & 0 & 0 & 0 \\ -\frac{7}{128} & \frac{105}{128} & \frac{35}{128} & -\frac{5}{128} & 0 & 0 & 0 & 0 \\ -\frac{5}{128} & \frac{35}{128} & \frac{105}{128} & -\frac{7}{128} & 0 & 0 & 0 & 0 \\ 0 & -\frac{7}{128} & \frac{105}{128} & \frac{35}{128} & -\frac{5}{128} & 0 & 0 & 0 \\ 0 & -\frac{5}{128} & \frac{35}{128} & \frac{105}{128} & -\frac{7}{128} & 0 & 0 & 0 \\ 0 & 0 & -\frac{7}{128} & \frac{105}{128} & \frac{35}{128} & -\frac{5}{128} & 0 & 0 \\ 0 & 0 & -\frac{5}{128} & \frac{35}{128} & \frac{105}{128} & -\frac{7}{128} & 0 & 0 \\ 0 & 0 & 0 & -\frac{7}{128} & \frac{105}{128} & \frac{35}{128} & -\frac{5}{128} & 0 \\ 0 & 0 & 0 & -\frac{5}{128} & \frac{35}{128} & \frac{105}{128} & -\frac{7}{128} & 0 \\ 0 & 0 & 0 & 0 & -\frac{7}{128} & \frac{105}{128} & \frac{35}{128} & -\frac{5}{128} \\ 0 & 0 & 0 & 0 & -\frac{5}{128} & \frac{35}{128} & \frac{105}{128} & -\frac{7}{128} \\ 0 & 0 & 0 & 0 & \frac{5}{128} & -\frac{27}{128} & \frac{135}{128} & \frac{15}{128} \\ 0 & 0 & 0 & 0 & \frac{7}{128} & -\frac{33}{128} & \frac{77}{128} & \frac{77}{128} \\ 0 & 0 & 0 & 0 & -\frac{15}{128} & \frac{65}{128} & -\frac{117}{128} & \frac{195}{128} \end{bmatrix}.$$

Consistent decimation matrix constructed using the local method (Section 4.2).

$$\tilde{H}^3_{local} = \begin{bmatrix} \frac{5}{16} & \frac{15}{16} & -\frac{5}{16} & \frac{1}{16} & 0 & 0 & 0 & 0 & 0 & 0 & 0 & 0 & 0 & 0 & 0 & 0 \\ \frac{1}{16} & -\frac{5}{16} & \frac{15}{16} & \frac{5}{16} & 0 & 0 & 0 & 0 & 0 & 0 & 0 & 0 & 0 & 0 & 0 & 0 \\ 0 & \frac{95}{2304} & -\frac{133}{2304} & -\frac{35}{256} & \frac{1505}{2304} & \frac{1505}{2304} & -\frac{35}{256} & -\frac{133}{2304} & \frac{95}{2304} & 0 & 0 & 0 & 0 & 0 & 0 & 0 \\ 0 & 0 & 0 & \frac{95}{2304} & -\frac{133}{2304} & -\frac{35}{256} & \frac{1505}{2304} & \frac{1505}{2304} & -\frac{35}{256} & -\frac{133}{2304} & \frac{95}{2304} & 0 & 0 & 0 & 0 & 0 \\ 0 & 0 & 0 & 0 & 0 & \frac{95}{2304} & -\frac{133}{2304} & -\frac{35}{256} & \frac{1505}{2304} & \frac{1505}{2304} & -\frac{35}{256} & -\frac{133}{2304} & \frac{95}{2304} & 0 & 0 & 0 \\ 0 & 0 & 0 & 0 & 0 & 0 & 0 & \frac{95}{2304} & -\frac{133}{2304} & -\frac{35}{256} & \frac{1505}{2304} & \frac{1505}{2304} & -\frac{35}{256} & -\frac{133}{2304} & \frac{95}{2304} & 0 \\ 0 & 0 & 0 & 0 & 0 & 0 & 0 & 0 & 0 & 0 & 0 & \frac{5}{16} & \frac{15}{16} & -\frac{5}{16} & \frac{1}{16} & 0 \\ 0 & 0 & 0 & 0 & 0 & 0 & 0 & 0 & 0 & 0 & 0 & \frac{1}{16} & -\frac{5}{16} & \frac{15}{16} & \frac{5}{16} & 0 \end{bmatrix}.$$

Consistent decimation matrix constructed using the global method (Proposition 1).

$$\tilde{H}^3_{global} = \begin{bmatrix} \frac{967}{3196} & \frac{229}{293} & \frac{1304}{4439} & -\frac{1514}{2775} & -\frac{442}{3725} & \frac{1453}{3514} & \frac{829}{39713} & -\frac{485}{2308} & \frac{17}{12480} & \frac{273}{3151} & \frac{23}{258095} & -\frac{414}{11815} & \frac{3}{538633} & \frac{85}{7874} & 0 & -\frac{55}{31813} \\ -\frac{122}{4263} & \frac{279}{293} & \frac{509}{1226} & \frac{487}{868} & \frac{114}{881} & -\frac{357}{2152} & -\frac{826}{55397} & \frac{77}{1007} & -\frac{17}{17472} & -\frac{127}{3939} & -\frac{8}{125681} & \frac{308}{23759} & -\frac{1}{251362} & -\frac{57}{14249} & 0 & \frac{22}{34369} \\ \frac{93}{3982} & \frac{40}{12017} & -\frac{178}{1477} & \frac{167}{4561} & \frac{869}{1582} & \frac{273}{466} & \frac{841}{18801} & -\frac{277}{1474} & \frac{17}{5824} & \frac{2312}{26423} & \frac{7}{36657} & -\frac{284}{8275} & \frac{3}{251362} & \frac{145}{13596} & \frac{1}{921661} & -\frac{39}{22936} \\ -\frac{101}{11369} & \frac{23}{105865} & \frac{107}{1835} & \frac{57}{23851} & -\frac{499}{2909} & \frac{269}{7035} & \frac{931}{1601} & \frac{972}{1663} & \frac{17}{448} & -\frac{3079}{16565} & \frac{17}{6848} & \frac{133}{1641} & \frac{11}{70897} & -\frac{457}{18680} & \frac{1}{70897} & \frac{23}{5808} \\ \frac{23}{5808} & \frac{1}{70897} & -\frac{457}{18680} & \frac{11}{70897} & \frac{133}{1641} & \frac{17}{6848} & -\frac{3079}{16565} & \frac{17}{448} & \frac{972}{1663} & \frac{931}{1601} & \frac{269}{7035} & -\frac{499}{2909} & \frac{57}{23851} & \frac{107}{1835} & \frac{23}{105865} & -\frac{101}{11369} \\ -\frac{39}{22936} & \frac{1}{921661} & \frac{145}{13596} & \frac{3}{251362} & -\frac{284}{8275} & \frac{7}{36657} & \frac{2312}{26423} & \frac{17}{5824} & -\frac{277}{1474} & \frac{841}{18801} & \frac{273}{466} & \frac{869}{1582} & \frac{167}{4561} & -\frac{178}{1477} & \frac{40}{12017} & \frac{93}{3982} \\ \frac{22}{34369} & 0 & -\frac{57}{14249} & -\frac{1}{251362} & \frac{308}{23759} & -\frac{8}{125681} & -\frac{127}{3939} & \frac{17}{17472} & \frac{77}{1007} & -\frac{826}{55397} & -\frac{357}{2152} & \frac{114}{881} & \frac{487}{868} & \frac{509}{1226} & \frac{279}{5470} & -\frac{122}{4263} \\ -\frac{55}{31813} & 0 & \frac{85}{7874} & \frac{3}{538633} & -\frac{414}{11815} & \frac{23}{258095} & \frac{273}{3151} & \frac{17}{12480} & -\frac{485}{2308} & \frac{829}{39713} & \frac{1453}{3514} & -\frac{442}{3725} & -\frac{1514}{2775} & \frac{1304}{4439} & \frac{229}{293} & \frac{967}{3196} \end{bmatrix}.$$

Compatible detail matrices constructed with $\tilde{H}^3_{local}$ (Proposition 2).

$$G^3_{local} = \begin{bmatrix}
1 & 0 & 0 & 0 & 0 & 0 & 0 & 0 \\
-\frac{3}{10} & \frac{1}{2} & 0 & 0 & 0 & 0 & 0 & 0 \\
0 & 1 & 0 & 0 & 0 & 0 & 0 & 0 \\
-\frac{1}{2} & -\frac{5}{2} & 0 & 0 & 0 & 0 & 0 & 0 \\
0 & 0 & 1 & 0 & 0 & 0 & 0 & 0 \\
-\frac{783}{9275} & -\frac{580}{1259} & -\frac{765}{757} & \frac{199}{1628} & -\frac{256}{4803} & -\frac{21}{4384} & -\frac{15}{38678} & -\frac{5}{361854} \\
0 & 0 & 0 & 1 & 0 & 0 & 0 & 0 \\
\frac{194}{13251} & \frac{237}{3635} & -\frac{716}{5987} & -\frac{1267}{1286} & \frac{288}{2591} & -\frac{78}{1439} & -\frac{77}{17546} & -\frac{9}{57560} \\
0 & 0 & 0 & 0 & 1 & 0 & 0 & 0 \\
\frac{144}{17005} & \frac{65}{1506} & \frac{1700}{42321} & -\frac{97}{793} & -\frac{1135}{1153} & \frac{745}{6636} & -\frac{89}{1826} & -\frac{25}{14396} \\
0 & 0 & 0 & 0 & 0 & 1 & 0 & 0 \\
\frac{10}{11789} & \frac{361}{73403} & \frac{91}{5703} & \frac{148}{4045} & -\frac{340}{2727} & -\frac{976}{1003} & \frac{1278}{7393} & -\frac{87}{4510} \\
0 & 0 & 0 & 0 & 0 & 0 & 1 & 0 \\
0 & 0 & 0 & 0 & 0 & 0 & -\frac{3}{10} & \frac{1}{2} \\
0 & 0 & 0 & 0 & 0 & 0 & 0 & 1 \\
0 & 0 & 0 & 0 & 0 & 0 & -\frac{1}{2} & -\frac{5}{2}
\end{bmatrix}$$

$$\tilde{G}^3_{local} \begin{bmatrix}
\frac{595}{1024} & -\frac{314}{181} & \frac{7065}{5186} & \frac{464}{1753} & -\frac{417}{1232} & -\frac{636}{1829} & \frac{662}{4535} & \frac{307}{2900} & -\frac{374}{10119} & -\frac{86}{12713} & \frac{68}{14073} & 0 & 0 & 0 & 0 & 0 \\
-\frac{105}{1024} & \frac{487}{2132} & \frac{65}{1822} & -\frac{439}{1195} & \frac{469}{3349} & \frac{227}{1586} & -\frac{161}{2962} & -\frac{296}{7853} & \frac{115}{8192} & \frac{86}{38139} & -\frac{98}{60845} & 0 & 0 & 0 & 0 & 0 \\
-\frac{5}{1024} & \frac{229}{2595} & -\frac{313}{1415} & \frac{171}{5446} & \frac{266}{577} & -\frac{577}{1062} & \frac{901}{6093} & \frac{188}{2263} & -\frac{484}{11719} & -\frac{13}{4118} & \frac{86}{38139} & 0 & 0 & 0 & 0 & 0 \\
\frac{5}{2048} & -\frac{104}{4429} & \frac{61}{1164} & \frac{64}{4059} & -\frac{173}{1318} & -\frac{767}{11946} & \frac{619}{1242} & -\frac{1006}{1907} & \frac{499}{3653} & \frac{188}{2263} & -\frac{484}{11719} & -\frac{13}{4118} & \frac{86}{38139} & 0 & 0 & 0 \\
0 & \frac{98}{60845} & -\frac{86}{38139} & -\frac{317}{19079} & \frac{484}{11719} & \frac{227}{7807} & -\frac{499}{3653} & -\frac{1225}{18432} & \frac{1}{2} & -\frac{1006}{1907} & \frac{499}{3653} & \frac{188}{2263} & -\frac{484}{11719} & -\frac{13}{4118} & \frac{86}{38139} & 0 \\
0 & 0 & 0 & \frac{98}{60845} & -\frac{86}{38139} & -\frac{317}{19079} & \frac{484}{11719} & \frac{227}{7807} & -\frac{499}{3653} & -\frac{199}{2896} & \frac{1036}{2059} & -\frac{389}{748} & \frac{65}{551} & \frac{179}{1815} & -\frac{209}{4105} & \frac{7}{2048} \\
0 & 0 & 0 & 0 & 0 & \frac{98}{60845} & -\frac{86}{38139} & -\frac{317}{19079} & \frac{484}{11719} & \frac{226}{3593} & -\frac{94}{511} & -\frac{467}{2582} & \frac{801}{1019} & -\frac{265}{344} & \frac{948}{3199} & -\frac{35}{1024} \\
0 & 0 & 0 & 0 & 0 & -\frac{86}{38139} & \frac{13}{4118} & \frac{141}{7787} & -\frac{435}{8596} & -\frac{177}{2494} & \frac{493}{2803} & \frac{1203}{7012} & -\frac{1000}{3801} & -\frac{496}{1269} & \frac{641}{1010} & -\frac{231}{1024}
\end{bmatrix}$$